Communication

Self-Assembly of Hexagonal DNA Two-Dimensional (2D) Arrays

Yu He, Yi Chen, Haipeng Liu, Alexander E. Ribbe, and Chengde Mao

J. Am. Chem. Soc., **2005**, 127 (35), 12202-12203• DOI: 10.1021/ja0541938 • Publication Date (Web): 12 August 2005

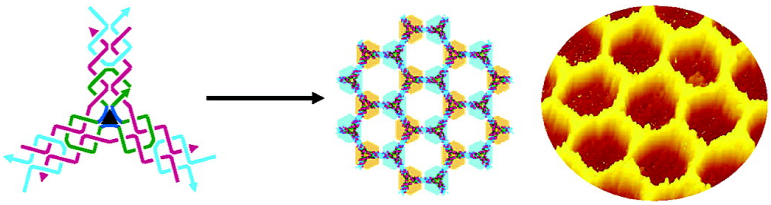

J|A|C|S
COMMUNICATIONS

Published on Web 08/12/2005

Self-Assembly of Hexagonal DNA Two-Dimensional (2D) Arrays

Yu He, Yi Chen, Haipeng Liu, Alexander E. Ribbe, and Chengde Mao*

Department of Chemistry, Purdue University, 560 Oval Drive, West Lafayette, Indiana 47907

Received June 24, 2005; E-mail: mao@purdue.edu

This paper reports a three-point-star DNA motif that can self-assemble into porous, hexagonal, two-dimensional (2D) arrays. The pores are hexagons, whose edges are ~18 nm long. The 2D DNA arrays are as large as 1 mm.

DNA is excellent for nanoconstruction because of its predictable structures and extraordinary molecular recognition.[1] DNA can organize nanoparticles[2a,b] and biomacromolecules,[2c] template nanofabrication,[3] and work as nanomachines.[4] A range of geometric, periodic, and dynamical nanostructures has been crafted out of DNA.[5] The success of such constructions relies on well-defined DNA construction motifs. However, the available DNA motifs are very limited and far behind the requirement to achieve technological complexity. Furthermore, current motifs have some intrinsic problems. For example, the domain sizes of the lattices assembled from those motifs are quite small, in many cases, narrower than 1 μm, as reported by our own group and other people.[5] This situation motivates us to search for more motifs with novel properties. Here, we report the design, construction, and self-assembly of a three-point-star DNA motif.

Figure 1 illustrates the structure of a three-point-star DNA motif. It consists of seven DNA single strands organized in three four-arm junctions (Figure 1a). Three T3 loops (dark blue lines) are located at the center to prevent helixes from stacking on one another. Junctions are related to each other by a 3-fold rotational symmetry and point from the center to peripheral. The overall shape is a three-point star. Individual four-arm junctions adopt flexible, nonplanar structure in the presence of divalent cations.[6] The three interconnected four-arm junctions in the three-point-star motif, however, constrain each other and force all component DNA duplexes to stay in one plane. Because of the 3-fold rotational symmetry, the seven component DNA strands are grouped into three identical red strands, three identical blue strands, and one green−dark blue strand. When proper sticky ends are added, the three-point-star motif will self-assemble into extended, hexagonal 2D arrays (Figure 1b). Even though the three-point-star motif is designed as a planar structure, it is still possible that the motif is not completely flat as designed. A corrugation strategy is used to ensure that arrays grow in one plane (Figure 1c).[7] With a corrugation strategy, any two neighboring units (three-point-star motifs here) are related by a 2-fold rotational axis and cancel each other's deviation from the plane. Such association, thus, allows nonperfectly planar units to assemble into planar 2D arrays. In the current design, each pseudo-continuing DNA duplex is 4.5 turns long (47 base pairs), which satisfies the corrugation requirement. To simplify the sequence design, two palindromic sequences are used for sticky ends. Because there is a 3-fold rotational symmetry, the same sticky ends are given to all three component junctions, which bring in an additional advantage. The cohesions between units in all directions are mediated by exactly the same sticky ends with exactly the same strength. Hence, isotropic arrays would be expected.

We followed experimental methods reported before.[5] Briefly, individual DNA strands were purified with denaturing polyacrylamide gel electrophoresis (PAGE), and DNA self-assembly was performed by slowly cooling mixtures containing equimolar component DNA strands from 90 to 4 °C (see Supporting Information for details). We first characterized the individual three-point-star motif with native PAGE (Figure 2). Each DNA complex appeared as a single, sharp band with expected mobility in the gel,

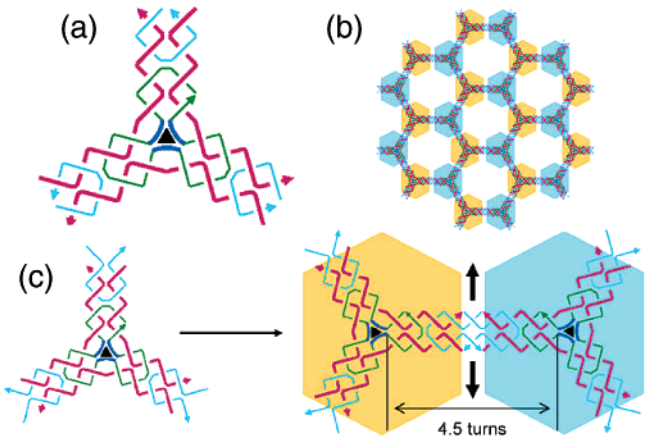

Figure 1. Three-point-star DNA motifs. (a) A blunt-ended DNA three-point star consists of three red strands, three blue strands, and one green−dark blue strand. The dark blue segments are T3 loops. A black triangle indicates a 3-fold rotational axis. (b) An extended, hexagonal 2D DNA array assembled from sticky-ended three-point stars. (c) Corrugated association of DNA three-point stars. Two interacting units (shadowed yellow or cyan) are related by a 2-fold rotational axis, indicated by arrowed black lines.

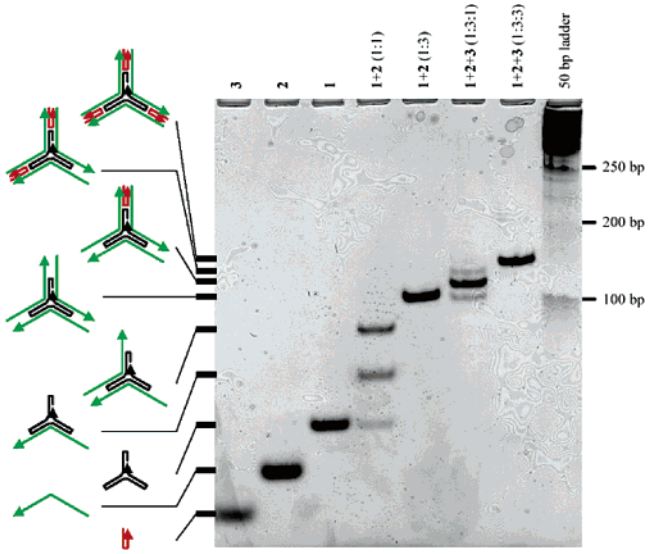

Figure 2. Native PAGE (6%) analysis of the individual three-point-star motif. DNA strands and their molar ratios (in parentheses) are indicated above the gel image, and the identities of all the bands are shown at the left side. The most right lane contains DNA duplex size markers.

10.1021/ja0541938 CCC: $30.25

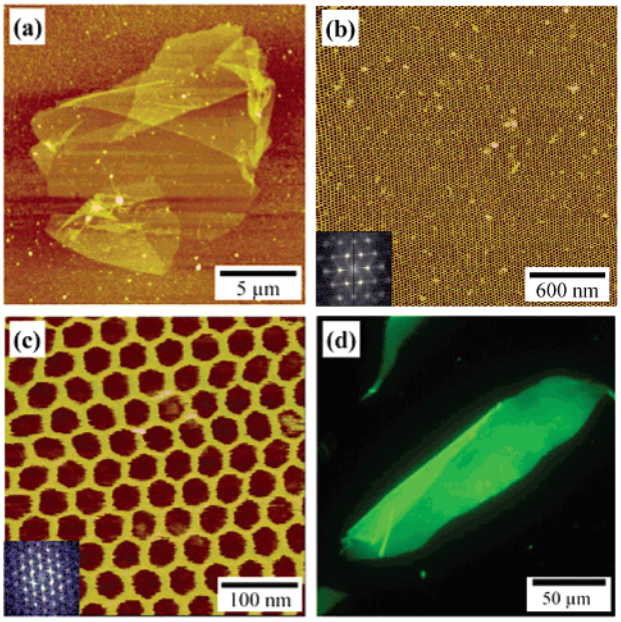

Figure 3. AFM and fluorescence imaging analysis of 2D crystalline DNA arrays self-assembled from three-point-star motifs with sticky ends. (a) A large domain of the DNA 2D lattice. (b) An AFM image with a small scanning area and (c) its zoom-in view. Insets are corresponding Fourier transform patterns. (d) A fluorescence image of a large DNA 2D lattice.

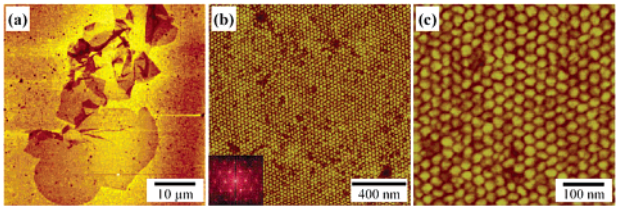

Figure 4. AFM analysis of gold replicas fabricated with the DNA 2D arrays as templates.

suggesting that the three-point-star complex formed and was stable under the experimental conditions.

With sticky ends, three-point-star motifs self-assembled into extended, hexagonal 2D crystalline arrays. The arrays are highly ordered, as judged by both direct observation and Fourier transform analysis of the atomic force microscopy (AFM) images (Figure 3a−c). The observed repeating distance was 29.9 ± 0.1 nm, in good agreement with the value (30.3 nm) calculated from the DNA model assuming 0.33 nm/base pair for the pitch and 2 nm for the diameter of a DNA duplex, respectively. The domain size of the 2D arrays reached 30 μm, and the domain was almost isotropic along all directions. We also imaged them with a fluorescence microscope. Compared with AFM, fluorescence microscopy was fast, convenient, and less destructive to DNA samples. DNA arrays as large as 1 mm were found (Figure 3d and Figure 1S in Supporting Information).

The resulting DNA arrays could be used as masks to fabricate metallic nanostructures with a protocol we developed before.[3b] A thin film of gold (20 nm thick) was vapor-deposited against the DNA lattices supported by mica and then mechanically lifted off. The gold film was a negative replica of the DNA structures (Figure 4). The hexagonal DNA patterns were accurately replicated into gold. Such fine, metallic nanopatterns are difficult to prepare by other means.

In summary, we have designed a three-point-star DNA motif that can self-assemble into large, hexagonal 2D lattices, which, in turn, can serve as a template to fabricate metallic nanostructures. Hexagonal DNA 2D arrays have been reported before;[5f,m] however, they either are not well-ordered or have only grown to around 1 μm in size. The design of the three-point-star motif was inspired by a cross motif,[5d] which can self-assemble into tetragonal 2D arrays. The success of the current design suggests that the design principle, first used by Yan et al.,[5d] might be generalized to design star motifs with any number of points, a family of geometric structures. Because the resulting lattices from this motif are large and stiff, at least two applications are possible. (i) The DNA lattices could potentially serve as ultrafine filters for nanofluidics and nanoparticle sorting. Particles can pass through these filters only if they are smaller than 30 nm, the size of the DNA pores. (ii) The DNA lattices could support biological particles (viruses or large protein complexes) for TEM imaging. Biological particles usually contain only light atoms and could not give good TEM contrast because the supporting films are usually thick (at least 20 nm). The reported DNA lattices are highly porous and only one molecular layer thin (~2 nm); thus, it would be expected to result in much higher contrast for the particles of interest.

Acknowledgment. This work was supported by the NSF (EIA-0323452), the DARPA/DSO (MDA 972-03-1-0020), and Purdue University (a start-up fund). AFM study was carried out in the Purdue Laboratory for Chemical Nanotechnology (PLCN).

Supporting Information Available: Experimental methods, DNA sequences, and additional fluorescence images. This material is available free of charge via the Internet at http://pubs.acs.org.

References

(1) For recent review on DNA self-assembly, see: Seeman, N. C. *Nature* **2003**, *421*, 427−431.
(2) (a) Alivisatos, A. P.; Johnsson, K. P.; Peng, X.; Wilson, T. E.; Loweth, C. J.; Bruchez, M. P.; Schultz, P. G. *Nature* **1996**, *382*, 609−611. (b) Mirkin, C. A.; Letsinger, R. L.; Mucic, R. C.; Storhoff, J. J. *Nature* **1996**, *382*, 607−609. (c) Niemeyer, C. M.; Sano, T.; Smith, C. L.; Cantor, C. R. *Nucleic Acids Res.* **1994**, *22*, 5530−5539.
(3) (a) Braun, E.; Eichen, Y.; Sivan, U.; Ben-Yoseph, G. *Nature* **1998**, *391*, 775−778. (b) Deng, Z.; Mao, C. *Angew. Chem., Int. Ed.* **2004**, *43*, 4068−4070.
(4) For reviews on DNA machines, see: (a) Seeman, N. C. *Trends Biochem. Sci.* **2005**, *30*, 119−125. (b) Simmel, F. C.; Dittmer, W. U. *Small* **2005**, *1*, 284−299. (c) Kelly, T. R. *Angew. Chem., Int. Ed.* **2005**, *44*, 4124−4127.
(5) (a) Winfree, E.; Liu, F.; Wenzler, L. A.; Seeman, N. C. *Nature* **1998**, *394*, 539−544. (b) LaBean, T. H.; Yan, H.; Kopatsch, J.; Liu, F.; Winfree, E.; Reif, J. H.; Seeman, N. C. *J. Am. Chem. Soc.* **2000**, *122*, 1848−1860. (c) Mao, C.; Sun, W.; Seeman, N. C. *J. Am. Chem. Soc.* **1999**, *121*, 5437−5443. (d) Yan, H.; Park, S. H.; Finkelstein, G.; Reif, J. H.; LaBean, T. H. *Science* **2003**, *301*, 1882−1884. (e) Liu, D.; Wang, M.; Deng, Z.; Walulu, R.; Mao, C. *J. Am. Chem. Soc.* **2004**, *126*, 2324−2325. (f) Ding, B.; Sha, R.; Seeman, N. C. *J. Am. Chem. Soc.* **2004**, *126*, 10230−10231. (g) Rothemund, P. W. K.; Papadakis, N.; Winfree, E. *PLoS Biology* **2004**, *2*, 2041−2053. (h) Shih, W. M.; Quispe, J. D.; Joyce, G. F. *Nature* **2004**, *427*, 618−621. (i) Malo, J.; Mitchell, J. C.; Venien-Bryan, C.; Harris, J. R.; Wille, H.; Sherratt, D. J.; Turberfield, A. J. *Angew. Chem., Int. Ed.* **2005**, *44*, 3057−3061. (j) Mathieu, F.; Liao, S.; Kopatsch, J.; Wang, T.; Mao, C.; Seeman, N. C. *Nano Lett.* **2005**, *5*, 661−665. (k) Park, S. H.; Barish, R.; Li, H.; Reif, J. H.; Finkelstein, G.; Yan, H.; LaBean, T. H. *Nano Lett.* **2005**, *5*, 693−696. (l) Chworos, A.; Severcan, I.; Koyfman, A. Y.; Weinkam, P.; Oroudjev, E.; Hansma, H. G.; Jaeger, L. *Science* **2004**, *306*, 2068−2072. (m) Chelyapov, N.; Brun, Y.; Gopalkrishnan, M.; Reishus, D.; Shaw, B.; Adleman, L. *J. Am. Chem. Soc.* **2004**, *126*, 13924−13925.
(6) (a) Murchie, A. I. H.; Clegg, R. M.; Vonkitzing, E.; Duckett, D. R.; Diekmann, S.; Lilley, D. M. J. *Nature* **1989**, *341*, 763−766. (b) Eis, P. S.; Millar, D. P. *Biochemistry* **1993**, *32*, 13852−13860.
(7) Yang, X.; Wenzler, L. A.; Qi, J.; Li, X.; Seeman, N. C. *J. Am. Chem. Soc.* **1998**, *120*, 9779−9786.

JA0541938